Design and Optimization of a Microstrip Bandpass Filter for Ultra Wideband (UWB) Wireless Communication

S. Seghier, N. Benabdallah, N. Benahmed, and K. Nouri

***Abstract*—A new technique is developed for designing a composite microstrip bandpass filter (BPF) with a -3dB fractional bandwidth of more than 100%. The BPF is suitable for ultra-wideband (UWB) wireless communications. The design utilizes embedding individually designed high-pass structures and low-pass filters (LPF) into each other, followed by an optimization for tuning in-band performance. The stepped-impedance LPF is employed to attenuate the upper stop-band and quarter-wave short-circuited stubs are used to realize the lower stop-band. The filter had a good performance, including an ultra-wideband bandpass (3-10 GHz), a small size, low insertion loss, return loss better than 18 dB from 3.8 GHz to 9.3 GHz and sharp rejection. The filter also demonstrated an UWB reject band from 11.4 GHz to more than 20 GHz at -20dB.**

***Index Terms*—Bandpass filters, microstrip lines, microstrip filters, ultra-wideband, wideband filters.**

I. Introduction

The ultra-wideband (UWB) wireless communication technology has received great attention, especially after the Federal Communications Commission (FCC) decision to permit the unlicensed operation band from 3.1 to 10.6 GHz in February 2002 [1]-[4].

The requirement of wideband bandpass filters (BPFs) has emerged from advance of the ultra-wideband (UWB) wireless communications [5], [6]. For the UWB purpose, the fractional bandwidth of BPFs usually exceeds 100%. Based on the traditional parallel-coupled line structure, very strong coupling structure will be a must for such a wide bandwidth. The tolerance of a microstrip fabrication process, however, imposes an upper limit upon coupling levels for coupling structures. To increase the coupling, special arrangement such as three-line structure [7] can be incorporated into the filter structure for wideband design. The relative bandwidths of the filters presented in [7], nevertheless, are still no more than 70%. Furthermore, filters synthesized using conventional method [8] show a smaller bandwidth than theoretical prediction, since the synthesis procedure is formulated only for relatively narrow band purposes [9]. Even the bandwidth prediction by sophisticated Q value distribution method [10] is promising; the implementation of the microstrip coupled stages with a very high coupling level is still limited by the resolution of fabrication process [11].

Alternatively, a wideband BPF can be constructed by a direct cascade of an LPF and an HPF. Both upper and lower transition bands can be determined individually as long as the input and output impedances of both filters are matched. In this paper, the HPF and the LPF are combined together, or equivalently one is embedded into the other, so that the circuit area of entire circuit can be greatly saved. A stepped-impedance structure is used to design the LPF because it is easier to design and occupies less space [9], [11]. Its design is readily available if the order, cutoff frequency, and in-band specification are specified. For realizing the HPF characteristic, i.e., the lower stopband, short-circuited stubs are tapped to the high-impedance microstrip sections of the LPF, so that attenuation poles are inserted at DC.

Optimization is then employed to fulfill the specification over a wide bandwidth. A filter with 3dB bandwidth of 107.69% is designed.

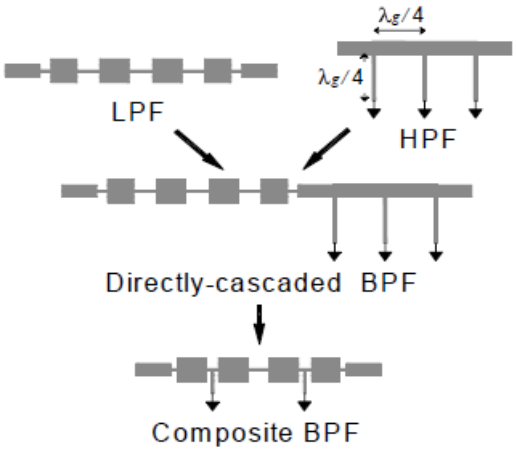

Fig. 1. Evolution of the composite BPF [11].

II. BPF Configuration and Design Procedure

Fig. 1 shows the configurations of a directly cascaded BPF and the composite BPF [11]. Obviously, the latter uses an area much less than the former. Both BPFs consist of a hi-Z, low-Z LPF and an HPF structure designed with shunt quarterwave short-circuited stubs separated with $\lambda_g/4$ sections, acting as impedance inverters. The variable λg is the guided wavelength at a proper frequency f_0 which will be addressed shortly.

Fig. 2(a) and 2(b) show the layouts of the microstrip LPF and HPF of our initial designs. The LPF has a cutoff frequency at 10 GHz, and the HPF at 3 GHz for fulfilling the UWB requirement.

Manuscript received February 9, 2016; revised July 5, 2016.

S. Seghier and K. Nouri are with the Laboratory of Technology and Communications, Department of Electronics, University Dr. Moulay Taher-Saida, BP 138 El- Naser 20000 Saida, Algeria (e-mail: seghier7@yahoo.fr, keltoum_nouri@yahoo.fr).

N. Benabdallah is with the Department of Physics, Preparatory School of Sciences and Technology, EPST-Tlemcen, Algeria (e-mail: N_Benabdallah@yahoo.fr).

N. Benahmed is with the Department of Telecommunications, University Abou Bekr Belkaid- Tlemcen, Algeria (e-mail: N_Benahmed@yahoo.fr).

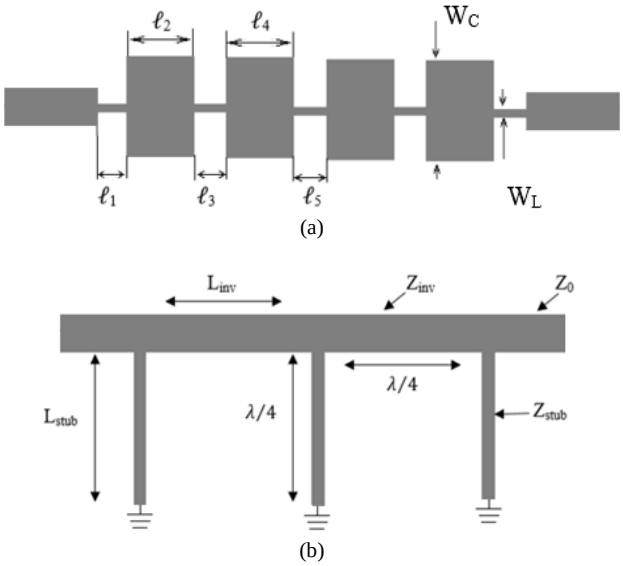

Fig. 2. (a) Geometry of LPF. ℓ_1 = 0.8168, ℓ_2 = 1.4767, ℓ_3 = 1.3027, ℓ_4 = 1.6549, ℓ_5 = 1.3331, W_C = 2.8176, W_L = 0.043 all in mm, (b) Geometry of HPF L_{stub} = 3.3075, L_{inv} = 2.7682, all in mm. Both circuits are symmetric about respective centers.

A. Stepped-Impedance LPF

In realization of a stepped-impedance LPF, the length of each line section is given as [9]:

$$\ell_L = \tan^{-1}\left(\frac{\omega_c L}{Z_{hi}}\right)\frac{v_c}{\omega_c\sqrt{\varepsilon_{hi,eff}}} \tag{1}$$

and

$$\ell_C = \sin^{-1}(\omega_c C Z_{low})\frac{v_c}{\omega_c\sqrt{\varepsilon_{low,eff}}} \tag{2}$$

where L and C are respectively the inductance and capacitance values of the LPF prototype scaled by the port impedance and cutoff frequency, v_c is the speed of light in free space, and ω_c represents the -3dB angular frequency. The effective dielectric constants $\varepsilon_{hi,eff}$ and $\varepsilon_{low,eff}$ are for the hi-Z and low-Z microstrip sections, respectively. The formulas can be simplified if each section is electrically short and the results are

$$\ell_L = \left(\frac{L}{Z_{hi}}\right)\frac{v_c}{\sqrt{\varepsilon_{hi,eff}}} \tag{3}$$

and

$$\ell_C = \frac{C Z_{low} v_c}{\sqrt{\varepsilon_{low,eff}}} \tag{4}$$

Note that all formulas (1) through (4) are derived with approximation. For initial design, one can use either (1) or (2) to implement L and either (3) or (4) to realize C. It is found that, based on our experience in this particular design, the synthesized LPF will have an accurate cutoff frequency and better agreement with an ideal LPF response by using (1) and (4). It could be due to the parasitic components existing in the impedance junctions [11].

The characteristic impedances for the sections have been selected as 130 Ω and 30 Ω respectively from [11].

Simulated S-parameters of the LPF are shown in Fig. 3. S-parameters were simulated using Advanced Design System (ADS) software. The filter is implemented on a substrate with dielectric constant ε_r = 10.8 and substrate height h = 1.27 mm.

Fig. 3. Simulated LPF performances.

B. High-Pass Filters

For the HPF in Fig. 2(b), the ABCD parameters of the impedance inverters and the shunt stubs are given as [9]:

$$\begin{bmatrix} A & B \\ C & D \end{bmatrix}_{inv} = \begin{bmatrix} \cos\left(\frac{\pi}{2}\frac{f}{f_0}\right) & jZ_{inv}\sin\left(\frac{\pi}{2}\frac{f}{f_0}\right) \\ jY_{inv}\sin\left(\frac{\pi}{2}\frac{f}{f_0}\right) & \cos\left(\frac{\pi}{2}\frac{f}{f_0}\right) \end{bmatrix} \tag{5}$$

and

$$\begin{bmatrix} A & B \\ C & D \end{bmatrix}_{stub} = \begin{bmatrix} 1 & 0 \\ \frac{-j}{Z_{stub}}\cot\left(\frac{\pi}{2}\frac{f}{f_0}\right) & 1 \end{bmatrix} \tag{6}$$

where Z_{inv} and Z_{stub} are the characteristic impedances of the inverter and stub, respectively.

From [11] and [12] the stub impedance was chosen to be 46 Ω and the inverter impedance was chosen to be 130 Ω.

Fig. 2(b). The complete design procedures of such are addressed in [9], [13], [14].

As we know this type of high pass filter shows a periodic response due to its distributed nature and it has a bandpass characteristic from DC up to 2 f_0 and a notch at 2 f_0.

So its center frequency must be large enough in order not to disturb the passband of our BPF. Hence the major point of designing the HPF for the proposed UWB filter is choosing f_0 [9], [13], [14]. This parameter determines the lengths of the short-circuited stubs and must be chosen in order to give a sufficient wide passband for our design. In this paper the stubs length are determined by choosing f_0 = 9 GHz.

The result of the high-pass filter (HPF) simulation is shown in Fig. 4.

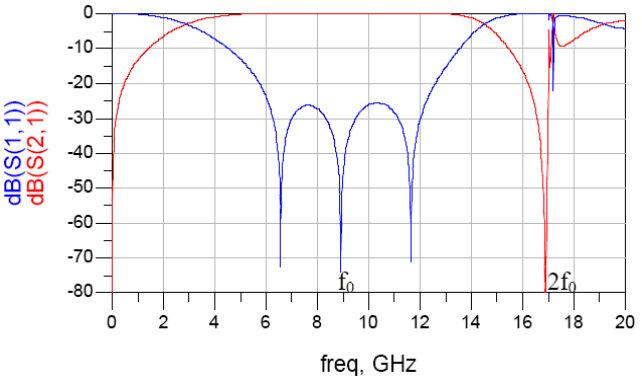

Fig. 4. Simulated HPF performances.

Both filters have return losses better than 15 dB in their respective passbands.

C. The Composite and the Directly Cascaded BPFs

The LPF and HPF shown in Fig. 2 can be directly cascaded (Fig. 5) or embedded each other to form a wideband BPF. Fig. 6 plots the geometry of the composite filter. In this circuit, two short-circuited stubs are used.

Fig. 7 compares the performances of these two BPFs. No optimization is applied to the directly cascaded filter, and its performance is used as a benchmark. Of the directly cascaded BPF, the upper and lower transition bands agree well with its counterparts shown in Fig. 3 and Fig. 4.

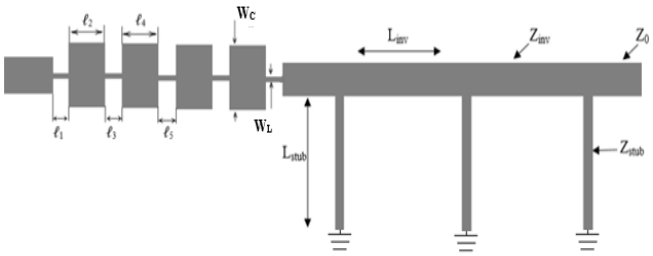

Fig. 5. Geometry of directly cascaded BPF.

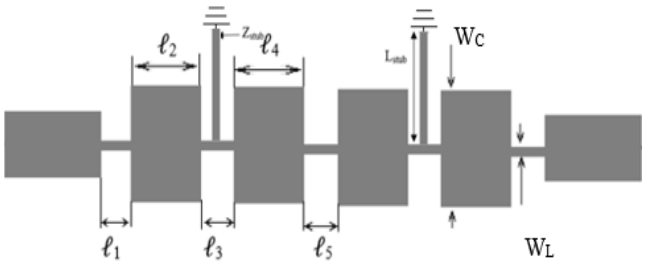

Fig. 6. Geometry of the composite BPF.

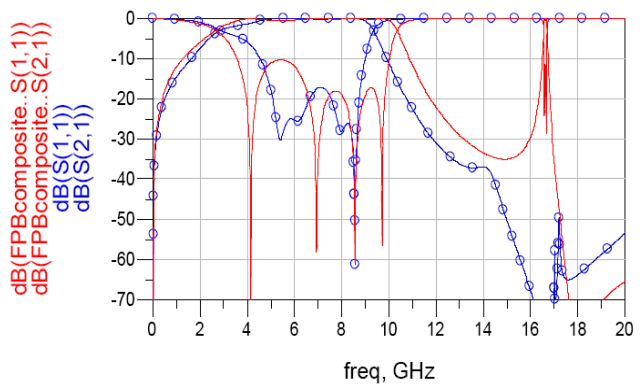

Fig. 7. Performances of the directly cascaded and the composite BPFs.

III. Optimal Design of the Composite BPF

To reach the specified request, we adopt the optimal design ability owning by ADS, numerical software based on the use of method of moments (MoM) [15], [16] (Fig. 6). We put the OPTIM controller in the schematic as well as three GOAL controllers to specify the optimal goals which we want to get after optimization. The paper sets two GOAL controllers which define the alias attenuation and reflect ratio respectively.

We use VAR components to set the tunable parameters such as microstrip width and length. In this design, the filter is symmetrical geometrically, indeed six group different values are needed to determine during the optimization. The parameters in the VAR component should set around the values which we have calculated with conventional method. As the composite filter is sensitive to the increment and decrease of its dimension, the value should not deflect the centre too much to lessen the time exhausted in the optimization.

The plot of the amplitude versus frequency after optimization is shown in Fig. 8. The passband is designed from 3 GHz to 10 GHz. The experimental circuit has not only a return loss better than 15 dB from 3.78 GHz to 9.3 GHz, but also a good rejection in the upper stopband 30dB at 20GHz.

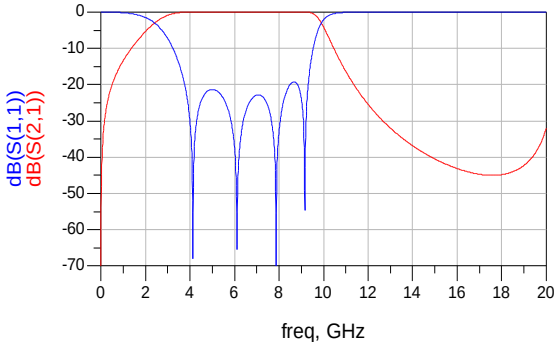

Fig. 8. Scattering parameters of the designed and optimized composite BPF.

After the optimization, we update the dimentions of the composite BPF with the new parameters which are derived from the optimization. The final refined parameters of the dimension are:

ℓ_1 = 0.5237, ℓ_2 = 1.621, ℓ_3 = 0.4711, ℓ_4 = 1.8638, ℓ_5 = 1.0563, L_{stub} = 2.5684, W_C = 3.7408, W_L = 0.032 all in mm.

IV. Conclusion

A new technique for designing microstrip BPFs suitable for the UWB wireless communications is proposed. The BPF is designed with a composite structure by embedding an HPF and an LPF to each other. The HPF is realized by coupled short-circuited stubs and the LPF is by the well-known stepped-impedance structure. Although the high-pass and low-pass structures in a composite BPF are perturbed by each other, the entire design shows a satisfactory bandpass characteristic over a wide bandwidth. this experimental filter is designed to have bandwidths complying with the upper frequency set and full-band of the UWB specifications.

The optimization function owning by ADS software is an

efficient tool to amend the drawback of conventional method with theoretic formulas.

REFERENCES

[1] Federal Communications Commission, "Revision of part 15 of the commission's rules regarding ultra-wideband transmission systems FCC," Tech. Rep., ET-Docket FCC02-48, Feb. 2002, pp. 98-153.

[2] T.-N. Kuo, C.-H. Wang, and C. H. Chen, "A compact ultra-wideband bandpass filter based on split-mode resonator," *IEEE Microwave and Wireless Components Letters*, vol. 17, no. 12, December 2007.

[3] Y. Saini and M. Kumar, "Ultra-wideband bandpass filter using short circuited stubs," *International Journal of Research & Technology*, vol. 3, issue 1, January 2014.

[4] M. Meeloon, "An ultra-wideband (UWB) bandpass filter multiple-notched band using embedded fold-slot structure," in *Proc. the 3rd International Conference on Industrial Application Engineering*, 2015.

[5] A. Saito, H. Harada, and A. Nishikata, "Development of bandpass filter for ultra wideband (UWB) communication systems," in *Proc. IEEE Conference on Ultra Wideband Systems and Technologies*, Nov. 2003, pp. 76–80.

[6] H. Ishida and K. Araki, "A design of tunable UWB filters," in *Proc. International Workshop on Ultra Wideband Systems*, May 2004, pp. 424-428.

[7] J.-T. Kuo and E. Shih, "Wideband bandpass filter design with three-line microstrip structures," in *Proc. 2001 IEEE MTT-S Int. Microwave Symp. Dig.*, pp. 1593-1596.

[8] K. S. Chin, L.-Y. Lin, and J.-T. Kuo, "New formulas for synthesizing microstrip bandpass filters with relatively wide bandwidths," *IEEE Microwave and Guided Wave Letters*, vol. 14, pp. 231-233, March 2004.

[9] D. M. Pozar, *Microwave Engineering*, New York: John Wiley & Sons, 2nd ed., 1998, ch. 8.

[10] J. M. Drozd and W. T. Joines, "Maximally flat quarter wavelength-coupled transmission-line filters using Q distribution," *IEEE Trans. Microwave Theory Tech.*, vol. 45, no. 12, pp. 2100-2113, Dec. 1997.

[11] C.-L. Hsu, F.-C. Hsu, and J.-T. Kuo, "Microstrip bandpass filters for UWB wireless communications," in *Proc. IEEE MTT-S Int. Symp. Dig.*, Jun. 2005, pp. 679-682.

[12] W. W. Mumford, "Tables of stub admittances for maximally flat filters using shorted quarter-wave stubs," *IEEE Trans. Microwave Theory Tech.*, vol. 13, pp. 373-376, Dec. 1965.

[13] J. S. Hong, *Microstrip Filter for RF/Microwave Applications*, A Wiley-Interscience Publication, Canada, 2001.

[14] M. Shobeyri and M. H. V. Samiei, "Compact ultra-wideband bandpass filter with defected ground structure," *Progress in Electromagnetics Research Letters*, vol. 4, pp. 25-31, 2008.

[15] Y. L. Hao, B. F. Zu, and P. Huang, "An optimal microstrip filter design method based on advanced design system for satellite receiver," in *Proc. IEEE International Conference on Mechatronics and Automation*, 2008.

[16] *Tuning, Optimization and Statistical Design*, Agilent Technologies, May 2003.

S. Seghier was born in Mecheria, Algeria. She received the doctor of ES-science degree from the University of Abou Bekr Belkaid Telmcen, Algeria in 2013. Since 2007, she has been an assistant professor of electronics in Dr. Moulay Tahar University, Saida, Algeria. Her current investigation concerns the RF and microwave components (filters, couplers…) used for telecommunication systems.

N. Benabdallah received the doctor of ES-science degree from the University of Tlemcen, Algeria in 2010. Since 2006, she has been an assistant professor of electronics in Preparatory School of Science and Techniques, EPST-Tlemcen. Her current investigation concerns the numerical characterization of the electromagnetic parameters of RF and microwave resonators using MoM and FEM for MRI applications.

N. Benahmed received the doctor of ES-science degree from the University of Tlemcen, Algeria in 2002. Since 2003, he has been a professor of communication systems. His current investigation concerns the RF and microwave circuits used for biomedical and telecommunication systems.

K. Nouri was born in Saida, Algeria. Her degree of bachelor in communication engineering was earned from Abou Bekr Belkaid in Telmcen, Algeria.

She is now an associate professor in Dr. Moulay Tahar University, Saida, Algeria. Her research interests are mainly in microwave technology: filters, couplers, attenuators, antennas.